

# Single step electrochemical synthesis of $\text{Sb}_2\text{Se}_3$ thin films: effect of molarities of precursor solution

P. M. Kulal · D. P. Dubal · V. J. Fulari

Received: 25 August 2010/Accepted: 3 December 2010/Published online: 23 December 2010  
© Springer Science+Business Media, LLC 2010

**Abstract** In the present investigation, we have successfully synthesized polycrystalline  $\text{Sb}_2\text{Se}_3$  thin films by single-step electrochemical method. Effect of concentration of precursor solution on structural, morphological, optical, and wettability properties by means of X-ray diffraction (XRD), scanning electron microscopy (SEM), optical absorption, and contact angle measurement have been investigated. It is evident from XRD pattern that  $\text{Sb}_2\text{Se}_3$  thin films are polycrystalline having orthorhombic crystal structure. Also, as precursor concentration increases the diffraction peak intensity also increases. Scanning electron micrographs reveal that the increase in precursor concentration causes the formation of soap foam like microstructure which is spread in the form of ellipsoids over whole substrate surface. The optical band gap decreases from 1.49 to 1.35 eV and contact angle decreases from  $40^\circ$  to  $13^\circ$ , i.e., the surface of  $\text{Sb}_2\text{Se}_3$  thin films converts from hydrophilic to superhydrophilic nature due to increase in precursor concentration. In addition, the holographic interferometric properties have been studied. The thickness, stress to substrate and deposited mass of the thin films is determined using double exposure holographic interferometry (DEHI) technique.

## Introduction

In recent years, considerable interest has been shown in the synthesis of thin semiconductor films by electrochemical

and chemical deposition of colloidal semiconductor [1]. Thin semiconducting films synthesized by electrochemical and chemical deposition methods are quite attractive for designing systems for electro-optics and photoelectrochemical (PEC) solar cells. These cells are simple in construction and have the advantages that they can be used for both photovoltaic and chemical energy conversions.

Recently, considerable attention has been given to the preparation and characterization of thin metal chalcogenide films by various techniques: pulsed laser deposition [2], antimony selenide via chemical bath deposition [3, 4], electrodeposition method [5, 6], spray pyrolysis technique [7], and SILAR method [8]. Among various selenides, antimony triselenide finds some special applications as target material of lithium-ion batteries [2] and photovoltaic cells [6, 7].

The double exposure holographic interferometry (DEHI) technique has been widely accepted as a viable tool for non-destructive testing of materials. This technique is sufficient to form a permanent record of relative surface displacement of object occurring after a fixed interval of time. As a result, the DEHI technique can be applied to many engineering problems, especially, continuous comparison of the surface displacement relative to an initial position [9]. The technique has been successfully employed to study the surface deformation of stainless steel (SS) with Ti–Ba–Ca–Cu thin film deposition [10].

Electrodeposition is very attractive method due to its potential advantages such as simple and easy control on the surface morphology. To the best of author's knowledge, there is no any report in which this different kind, i.e., soap foam like morphology investigated. Also, there is no any single report on DEHI technique to calculate different surface properties (thickness, stress to substrate, and deposited mass).

P. M. Kulal · D. P. Dubal · V. J. Fulari (✉)  
Holography and Material Research Laboratory, Department of Physics, Shivaji University, Kolhapur 416004, India  
e-mail: vijayfulari@gmail.com

In the present work, we report on single-step electro-synthesis of polycrystalline  $\text{Sb}_2\text{Se}_3$  thin films. Effect of concentrations of precursor solution on structural, morphological, optical, and wettability properties have been investigated. In addition, the holographic interferometric properties have been studied. The thickness and stress of the films have been determined by DEHI technique for various concentrations.

## Experimental

### Preparation of $\text{Sb}_2\text{Se}_3$ thin film

The electrodeposition of  $\text{Sb}_2\text{Se}_3$  thin films was carried out from an electrolyte bath consisting of potassium antimony tartarate and selenium dioxide ( $\text{SeO}_2$ ) aqueous solutions. All solutions were prepared immediately prior to each experiment by dissolving the requisite amounts of analytical reagent grade salts in double distilled water. The concentration of the antimony precursor solution was varied from 0.05 to 0.1 M at an interval of 0.025 M by changing the amount of potassium antimony tartarate dissolved in double distilled water. The pH of the bath was maintained to  $\sim 3$ . The used SS substrates were mirror polished with zero grade polish paper, cleaned with detergent and finally cleaned ultrasonically. A graphite plate was used as a counter electrode. All the potentials were measured with respect to SCE. The cathode to anode distance was 0.5 cm. Electrodeposition was carried out potentiostatically using a constant voltage source. The deposition conditions were optimized to get good quality  $\text{Sb}_2\text{Se}_3$  films of maximum thickness. The prepared  $\text{Sb}_2\text{Se}_3$  films were found to be well-adherent uniform and grayish in color.

The  $\text{Sb}_2\text{Se}_3$  thin films were analyzed by X-ray diffraction (XRD) within the range 10–100° on computer controlled Philips PW-3710 using Cr  $K_\alpha$  radiations ( $\lambda = 2.2897 \text{ \AA}$ ) to determine the film structures. Microstructural study was carried out using scanning electron microscopy (SEM-JEOL 6360). The optical absorption study was carried out over the wavelength range 400–1500 nm using UV–Vis–NIR spectrophotometer, with FTO substrate as a reference. For the surface wettability test, contact angle measurement based on the sessile-drop method consisting of the observation of water drop through a comprising microscope coupled to goniometer was preferred. A 2 mL drops were sequentially deposited at different surface positions on the film using a Rame-Hart Inc. model-10 micro-syringe. Contact angles were determined after 10 s of stability period. This time is necessary for focusing and adjusting the crosshairs of the microscope on the drop.

### Double exposure holographic interferometry technique

Holograms are recorded using double exposure holographic interferometry technique. The holograms were recorded by conventional two beam off-axis technique using 10 mW He–Ne laser having wavelength  $\lambda = 6328 \text{ \AA}$ . The holograms were recorded on the holographic film (Kodak 8E 75 HD) before and after the deposition of  $\text{Bi}_2\text{Se}_3$  thin films. The reconstructed image of substrate was observed with the reference beam which shows the localized fringes.

### Measurement of thickness of the films and stress to the substrate

The simple non-destructive technique, for the quantitative measurement of stress in thin films by the use of DEHI technique is reported by [11]. While recording the hologram, if the object is illuminated with a beam of light making an angle  $\theta_1$  with the normal and is viewed at an angle  $\theta_2$  during reconstruction, the reconstructed image has a superimposed fringe pattern corresponding to a displacement of the surface. The displacement in the normal direction is given by

$$d = \frac{n\lambda}{\cos \theta_1 + \cos \theta_2}, \quad (1)$$

where  $n$  is the number of fringes and  $\lambda$  is the wavelength of light. In general,  $\theta_1$  and  $\theta_2$  are sufficiently small, so that

$$d = \frac{n\lambda}{2}$$

The stress to the stainless substrate is given by the formula [12]

$$s = \frac{t_s^2 Y_s \Delta}{3l^2 t_f}$$

where,  $S$  is the stress in dyne/cm<sup>2</sup>,  $t_s$  is the substrate thickness,  $t_f$  is the film thickness,  $\Delta$  is the deflection of the substrate equal to  $4\lambda/2$ ,  $Y_s$  is the Young's modulus,  $l$  is the length of the substrate on which the film is deposited. The mass of the deposited film was calculated using the relation

$$\text{Mass} = \text{density} \times \text{volume}$$

## Results and discussion

### Cyclic voltammetry

Cyclic voltammetry was used to monitor the electrochemical reactions in solutions of 0.1 M  $[\text{K}(\text{SbO})\text{C}_4\text{H}_4\text{O}_6] + 0.1 \text{ M SeO}_2 + 0.1 \text{ M EDTA}$  to find the suitable  $\text{Sb}_2\text{Se}_3$  deposition potential. All voltammetry curves

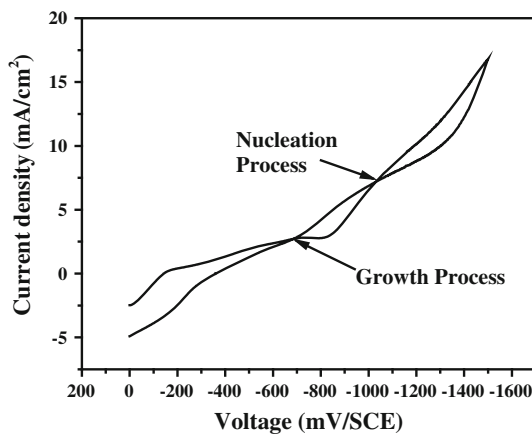


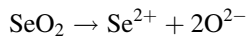
**Fig. 1** Cyclic voltammogram on stainless steel substrate in the solution containing 0.1 M  $[K(SbO)_2 \cdot C_4H_4O_6 + SeO_2 + EDTA]$

were scanned first in the cathodic direction and the current density indicates a cathodic current.

Figure 1 shows the cyclic voltammograms measured for the SS electrode in the electrolytic bath of 0.1 M  $[K(SbO)_2 \cdot C_4H_4O_6] + 0.1 M SeO_2 + 0.1 M EDTA$ . It is clearly seen that the cathodic current increases sharply from  $-0.83 V/SCE$ , which belongs to simultaneous reduction of both antimony and selenium ions. The films deposited at  $-0.85 V/SCE$  potential are homogenous, uniform, and well-adherent to the substrates. The crossover between anodic and cathodic current curves appears on the reverse potential sweep which indicates that nucleation and growth process exist on the substrate in electrolytic bath.

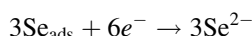
#### Film formation and reaction mechanism

Electrodeposition of  $Sb_2Se_3$  was carried out from aqueous acidic bath. The  $Sb_2Se_3$  films were cathodically deposited from an aqueous solution containing antimony and selenium ions. The electrodeposition of  $Sb_2Se_3$  had been carried out from an aqueous acidic solution containing antimony and selenium ions.

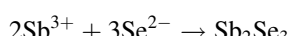


$SeO_2+$  is converted into  $Se_{ads}$ .

The electron reacts with  $Se_{ads}$ .



A complex of  $Sb^{3+}$  reacts with  $Se^{2-}$  to give



#### Structural study

Figure 2a–c shows the XRD patterns of  $Sb_2Se_3$  thin films deposited for three different concentrations 0.05, 0.075, and 0.1 M, respectively. With increasing the concentration

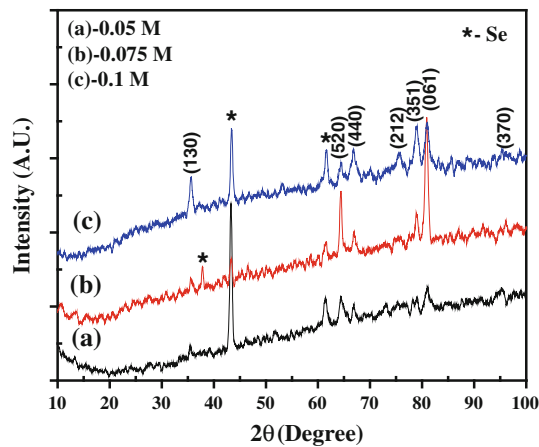


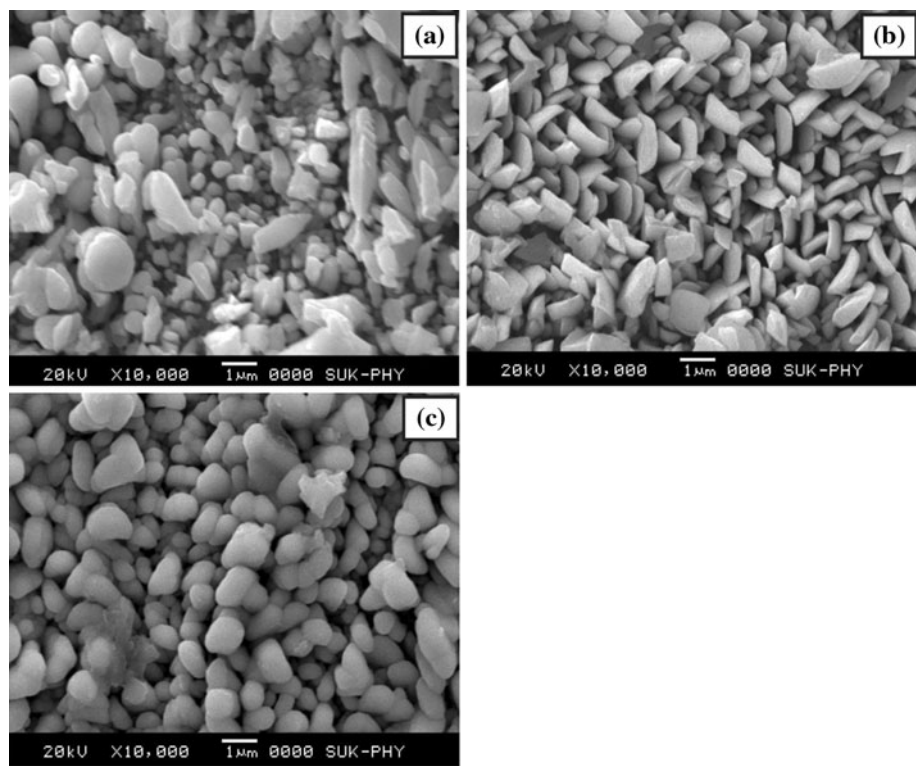
**Fig. 2** The X-ray diffraction patterns of  $Sb_2Se_3$  thin films for three different precursor concentrations: (a) 0.05 M, (b) 0.075 M, and (c) 0.1 M

of precursor solution, increase in film thickness was observed. This may be due to sufficient reaction time period available for the formation of oriented growth of  $Sb_2Se_3$  thin films along specific plane. It is evident from XRD pattern that  $Sb_2Se_3$  thin films are polycrystalline having orthorhombic crystal structure. Similar type of results has been reported elsewhere [4, 6]. The XRD pattern indicates the presence of (130), (520), (440), (212), (351), (061), and (370) planes of  $Sb_2Se_3$  materials, which is in good agreement with JCPDS cards no. 01-075-1462. In XRD pattern, Se phase is also observed which may be due to the higher concentration of  $SeO_2$ . It should be noted that the relative peak intensity of the diffraction arising from all the peaks increases with increase in concentration of precursor solution. The diffraction peaks marked by \* are due to selenite.

#### Surface morphological studies

The surface morphology of the  $Sb_2Se_3$  thin films for different concentration of precursor solution were shown in Fig. 3a–c at  $10,000\times$  magnification. Observed surface morphology for 0.05 M concentration suggest a uniform growth of first few layers of  $Sb_2Se_3$  nanocrystallites and as the growth proceeds agglomeration of grains takes place, giving non-uniformity in grain size on surface of the thin film (Fig. 3a). However, the increase in precursor concentration to 0.075 M governs vertical growth of  $Sb_2Se_3$  so as to form vertically patterned arrays of  $Sb_2Se_3$  nanocrystallites (Fig. 3b). In this case, the surface of  $Sb_2Se_3$  thin films rough, porous, and nanocrystallites are uniformly spread over the whole surface. Further, increase in precursor concentration to 0.1 M completely destroys the previously developed surface morphologies. Now the surface of  $Sb_2Se_3$  thin films looks like soap foam which is

**Fig. 3** Scanning electron micrograph (SEM) images ( $10,000\times$ ) of  $\text{Sb}_2\text{Se}_3$  thin films for three different precursor concentrations: **a** 0.05 M, **b** 0.075 M, and **c** 0.1 M



spread in the form of ellipsoids over whole substrate surface as seen from Fig. 3c. This morphological change is attributed may be due to the presence of excess antimony in atomic percentage [13].

#### Optical studies

The variation of optical band gap of  $\text{Sb}_2\text{Se}_3$  films for three different precursor concentrations is shown in Fig. 4. This data was further used for analyzing optical direct band gap energy using following classical relation for near edge

optical absorption in semiconductor. The theory of optical absorption gives the relationship between the absorption coefficient  $\alpha$  and the photon energy ' $h\nu$ ' can be written as

$$\alpha = \frac{A(E_g - h\nu)^n}{h\nu}, \quad (5)$$

where  $\alpha$  is the absorption coefficient,  $A$  is a constant,  $E_g$  is the band gap, and  $n$  is equal to 1/2 for a direct and 2 for indirect transition. Figure 3 shows the plots of  $(\alpha h\nu)^2$  versus  $h\nu$  plotted for estimating the values of direct band gap energy of  $\text{Sb}_2\text{Se}_3$  films by extrapolating curves to zero absorption coefficient. The band gap energy ( $E_g$ ) values are found to be 1.49, 1.38, and 1.35 eV for 0.05, 0.075, and 0.1 M precursor concentrations, respectively, which are slightly greater than earlier reported values [6]. The decrease in band gap energy may be attributed to increased grain size [14, 15]. Table 1 shows the comparison of band gap with earlier reported values.

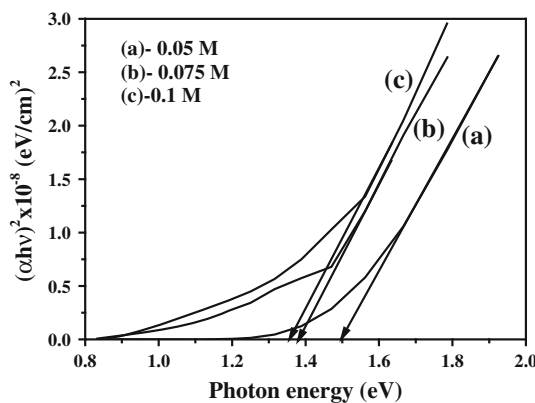


**Fig. 4** The variation of  $(\alpha h\nu)^2$  with photon energy ( $h\nu$ ) of  $\text{Sb}_2\text{Se}_3$  thin films for three different precursor concentrations: (a) 0.05 M, (b) 0.075 M, and (c) 0.1 M

**Table 1** Comparison of band gap values with earlier reported values

S. no.	Method	Band gap	Reference
1.	Microwave-assisted $\text{Sb}_2\text{Se}_3$	1.16–1.17	[20]
2.	Microwave-assisted $\text{Sb}_2\text{Se}_3$	1.16	[21]
3.	Electrodeposited $\text{Sb}_2\text{Se}_3$	2.0	[6]
4.	Thermal evaporation $\text{Sb}_2\text{Se}_3$	1.29	[22]
5.	Chemical bath deposition $\text{Sb}_2\text{Se}_3$	1.11–1.19	[3]

### Wettability test

Wettability test is carried out in order to investigate the interaction between liquid and  $\text{Sb}_2\text{Se}_3$  thin films. If the wettability is high, contact angle ( $\theta$ ), will be small and the surface is hydrophilic. On the contrary, if the wettability is low,  $\theta$  will be large and the surface is hydrophobic. A contact angle of  $0^\circ$  means complete wetting and a contact angle of  $180^\circ$  corresponds to complete non-wetting. Both super-hydrophilic and super-hydrophobic surfaces are important for practical applications [16]. From Fig. 5, we observed that the  $\text{Sb}_2\text{Se}_3$  thin films are hydrophilic as water contact angle is  $40^\circ$  ( $<90^\circ$ ) means high wettability. As the

concentration of precursor solution increases the water contact angle decreases. The contact angles for 0.075 and 0.1 M concentration was found to be  $25^\circ$  and  $13^\circ$ . This may be due to the strong cohesive force between the water droplet and hydroxide present in the  $\text{Sb}_2\text{Se}_3$  compound. Similar type of behavior has been reported by More et al. [17] for chemically deposited  $\text{TiO}_2$  thin films. Thus, as concentrations of precursor solution increases the surface of  $\text{Sb}_2\text{Se}_3$  thin films converts from hydrophilic to super-hydrophilic nature. This specific property is attributed to nanocrystalline nature that is expected to possess very high surface energy. Due to which the water is attracted rather repelled by the  $\text{Sb}_2\text{Se}_3$  film. This specific property is useful for making intimate contact of aqueous electrolyte with electrode surface in PEC cell.

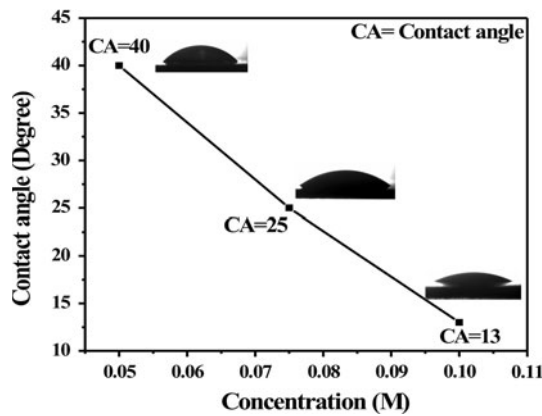
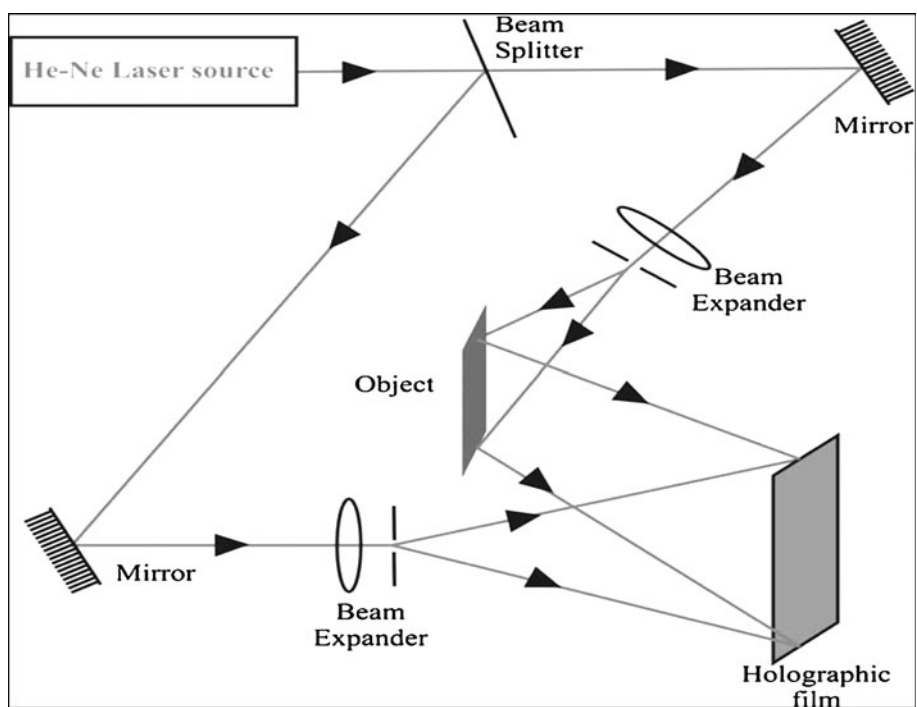


**Fig. 5** Contact angles of  $\text{Sb}_2\text{Se}_3$  thin films for three different precursor concentrations: (a) 0.05 M, (b) 0.075 M, and (c) 0.1 M

### Double exposure holographic interferometry

The actual experimental setup of double exposure holographic interferometry technique is shown in Fig. 6. The recorded holograms of  $\text{Sb}_2\text{Se}_3$  thin films deposited onto SS substrate at different concentrations of electrolyte are shown in Fig. 7. From the hologram study (Fig. 8), it is observed that as the bath concentration increases, the number of fringes localized on the surface of SS substrate goes on increasing [18]. From the Figs. 9, 10, and 11, it is observed that thickness increases deposited mass increases and stress to the substrate decreases with increasing bath concentration, respectively, as shown in Table 2. Janseen et al. reported that decrease in CrN thin film stress with

**Fig. 6** Actual experimental setup of the double exposure holographic interferometry technique



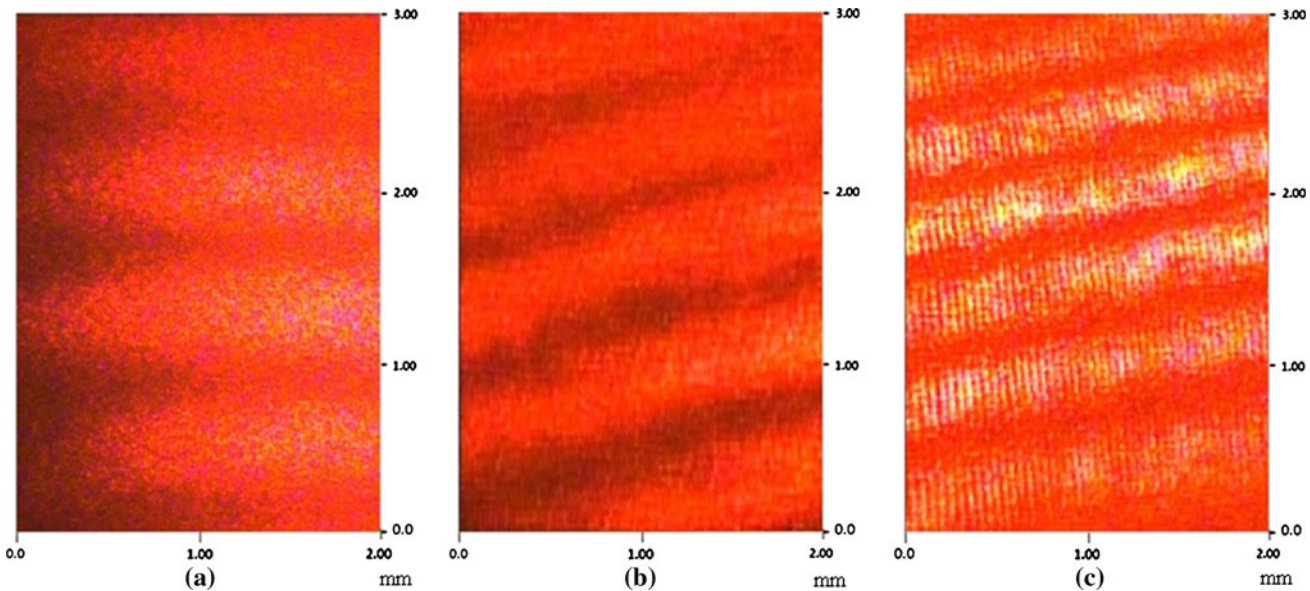


**Fig. 7** Recorded holograms of  $\text{Sb}_2\text{Se}_3$  thin films at different concentration: **a** 0.05 M, **b** 0.075 M, and **c** 0.1 M

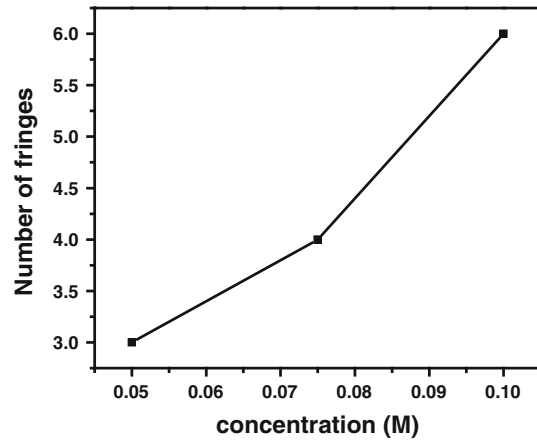


**Fig. 8** No. of fringes with at different concentration: **(a)** 0.05 M, **(b)** 0.075 M, and **(c)** 0.1 M

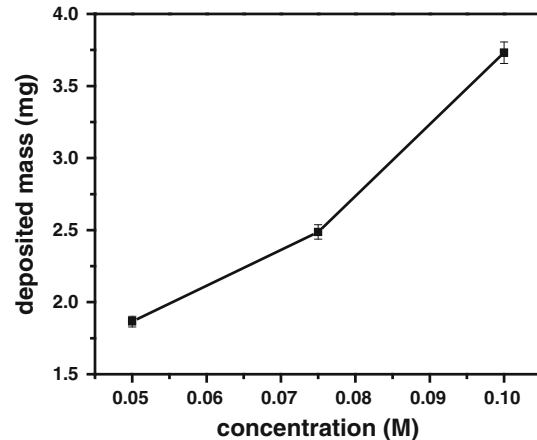


**Fig. 10** The variation of  $\text{Sb}_2\text{Se}_3$  film deposited mass at different concentration: **(a)** 0.05 M, **(b)** 0.075 M, and **(c)** 0.1 M

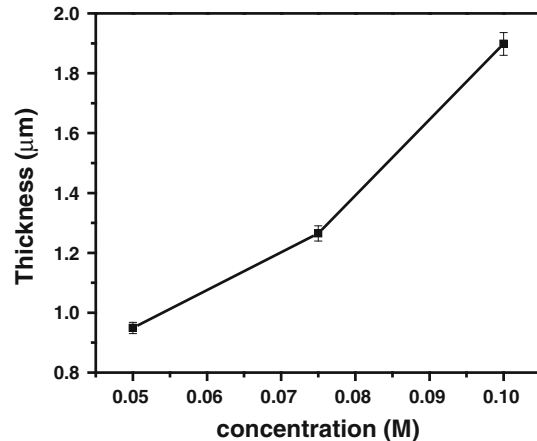


**Fig. 9** The variation of  $\text{Sb}_2\text{Se}_3$  film thickness with at different concentration: **(a)** 0.05 M, **(b)** 0.075 M, and **(c)** 0.1 M

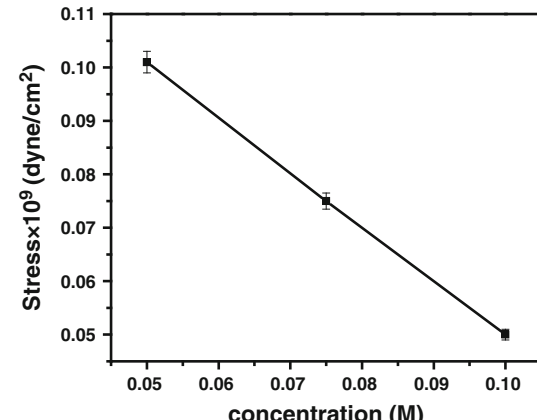


**Fig. 11** The variation of  $\text{Sb}_2\text{Se}_3$  film stress to substrate with at different concentration: **(a)** 0.05 M, **(b)** 0.075 M, and **(c)** 0.1 M

**Table 2** The observed number of fringes, thickness, stress to the substrate, and mass deposited for various bath concentration

Bath conc. (M)	Deposition time (h)	Fringe numbers	Thickness of film (μm)	Mass deposited (mg)	Stress × 10 <sup>9</sup> (dyne/cm <sup>2</sup> )
A = 0.05	1	3	0.949	1.865	0.101
B = 0.075	1	4	1.265	2.487	0.075
C = 0.1	1	6	1.898	3.731	0.050

thickness [19]. This may be due to scattering or interference of incident light.

## Conclusions

In summary, we have successfully synthesized polycrystalline Sb<sub>2</sub>Se<sub>3</sub> thin films by simple and inexpensive electrodeposition method. From scanning electron micrograph images, it is seen that there is significant change due to the change in the concentration of precursor solution. The optical band gap decreases from 1.49 to 1.35 eV and contact angle decreases from 40° to 13°, i.e., the surface of Sb<sub>2</sub>Se<sub>3</sub> thin film converts from hydrophilic to superhydrophilic nature due to increase in precursor concentration. In addition, the holographic interferometric properties have been studied. The thickness, stress to substrate and deposited mass of the thin films is determined using DEHI technique.

**Acknowledgement** Authors are grateful to the University Grants Commission (UGC), New Delhi for financial support through the scheme no. 36-209/2008 (SR).

## References

- El-wahabb EA, Fouad SS, Fadel M (2003) J Mater Sci 38:527. doi:[10.1023/A:1021863605287](https://doi.org/10.1023/A:1021863605287)
- Xue MZ, Fu ZW (2008) J Alloys Compd 458:351
- Lazcano YR, Pen Y, Nair MTS, Nair PK (2005) Thin Solid Films 493:77
- Lokhande CD, Sankapal BR, Saratale SD, Pathan HM, Giersig M, Ganesan V (2002) Appl Surf Sci 193:1
- Torane AP, Bhosale CH (2002) J. Phys. Chem. Solids 63:1849
- Fernandez AM, Merino MG (2000) Thin Solid Films 366:202
- Rajpure KY, Bhosale CH (2002) Mater Chem Phys 73:6
- Lokhande CD, Sankapal BR, Mane RS, Pathan HM, Muller M, Giersig M, Ganesan V (2001) Appl Surf Sci 182:413
- Dongare MB, Fulari VJ, Thokale RN, Kulkarni HR (1999) Asian Chem Lett 3:52
- Thokale RN, Patil PS, Dongare MB (2002) Mater Chem Phys 74:143
- Magill PJ, Young T (1967) J Vac Sci Technol 4:47
- Pawar SJ, Chikode PP, Fulari VJ, Dongare MB (2007) Mater Sci Eng B 137:23
- Ristic M, Popovic S, Music S (2004) Mater Lett 58:2494
- Kale SS, Mane RS, Pathan HM, Shaikh AV, Joo OS, Han SH (2007) Appl Surf Sci 253:4335
- Pathan HM, Kale SS, Lokhande CD, Han SH, Joo OS (2007) Mater Res Bull 42:1565
- Sun RD, Nakajima A, Fujushima A, Watanabe T, Hashimoto K (2001) J Phys Chem B 105:1984
- More AM, Gunjkar JL, Lokhande CD, Mane RS, Han SH (2007) Micron 38:500
- Fulari VJ, Malekar VP, Gangawane SA (2010) Prog Electromagn Res C 12:53
- Janseen GCAM, Tichelaar FD, Visser CCG (2006) J Appl Phys 100:093512
- Guo L, Ji G, Chang X, Zheng M, Shi Y, Zheng Y (2010) Nanotechnology 21:035606
- Zhou B, Zhu JJ (2009) Nanotechnology 20:085604
- ElSayad EA, Moustafa AM, Marzouk SY (2009) Physica B 404:1119